Journal of Marine Research, 47, 411–440, 1989

Open-incubation, diffusion methods for measuring solute reaction rates in sediments

by Robert C. Aller[1] and James E. Mackin[1]

ABSTRACT

Sedimentary solute distributions and fluxes are determined in part by the kinetics of production/consumption reactions in a deposit. It is possible to estimate rates and investigate kinetic relations in undisturbed or manipulated sediments by documenting build-up or depletion patterns of solutes allowed to diffuse either between relatively thin sections of sediment and a well-stirred water reservoir (plug incubation); or through a large section of sediment without an overlying reservoir (whole-core incubation). The time-dependent concentrations in the sediment in both cases depend on reaction rates, kinetics, diffusion coefficients, and geometric scaling of the sediment and contacting reservoir. Major advantages of the plug incubation method are that interactions between classes of sedimentary reactions can be examined by manipulating the composition of the stirred water reservoir, and kinetic relations, such as reaction order, can be inferred from comparisons of reaction rate with steady-state concentrations of pore water solutes. The water reservoir size and sediment thickness can be altered to allow rapid estimates of reaction rates at near steady-state or to examine nonsteady-state behavior. Nonsteady-state models are always required for the whole-core incubation method. This latter method has the advantages that it is less labor-intensive than many other rate measurement methods and the incubations can be performed *in situ*. Experimental comparisons between open-incubation and more traditional closed-incubation estimates of reaction rates show good agreement for solutes such as NH_4^+, $SO_4^=$, $HPO_4^=$ and I^-. In some cases, such as Mn^{++}, Fe^{++}, and $HPO_4^=$ production, where major back-reactions with sediment occur, open-incubations without substantial build-up of solutes may provide the most accurate method for estimating production rates. In principle, the open incubation methods described in this paper can be used for any diffusable species.

1. Introduction

The accurate interpretation of solute distributions, fluxes, and cycles within sedimentary deposits requires knowledge of the rates of solute consumption or production reactions. The most common methods of estimating reaction rates are: (1) calculating reaction rates necessary to reproduce the observed natural distributions over the region of interest by using a transport-reaction model (Berner, 1980); (2) isolating a portion of a deposit and directly following subsequent time-dependent net concentration changes during closed incubation (Martens and Berner, 1974; Goldha-

1. Marine Sciences Research Center, SUNY at Stony Brook, Stony Brook, New York, 11794-5000, U.S.A.

ber *et al.*, 1977); and (3), internal addition of an appropriate isotope to trace net/gross reaction rates in the pore water reservoir (Jorgensen, 1977; Blackburn, 1979).

Although these are powerful and useful methods, some disadvantages are that the natural transport and boundary conditions may not be properly characterized; reactions may have complex spatial variation; closed systems may produce concentration-dependent artifacts under certain conditions; serial incubations are often time-consuming and large samples may be required; and isotopic tracers are not available for all solutes. In this paper, we describe two alternative open-system methods for estimating reaction rates and investigating kinetics. We present the theory involved, and discuss advantages and limitations of both methods. The methods represent conceptual hybrids between field-based transport-reaction models of natural distributions and laboratory incubation methods. They are modifications and/or generalizations of experimental approaches that have been reported previously (e.g. Aller, 1978; Keir, 1983; Kelly, 1983; Burdige and Kepkay, 1983; Mackin, 1987).

2. Methods and theory

a. Plug incubation

The basic principle in the plug incubation method is to expose the surface of a sediment slice or plug of fixed thickness to a well-stirred water reservoir of fixed volume (Fig. 1). In many practical cases where anoxic sediment is used, the water reservoir is maintained anoxic by continual purging with, for example, N_2/CO_2 or by storage in a larger anoxic enclosure. Diffusive exchange of solutes occurs between the sediment pore water and overlying water reservoirs. The water compositions in each reservoir as a function of time are determined in part by production or consumption rates of sedimentary solutes as well as appropriate diffusion coefficients and geometric scaling. As a result, there are two basic measures of a solute's average production/consumption rate in the sediment: (1) the pore water solute concentration profile at any given time after exposure and (2), the flux of the solute out of or into the sediment plug. In the form of the method described here, the sediment thickness is sufficiently small relative to spatial variation in reaction rates that measurement of only a single averaged pore water concentration, rather than a complete profile, is used in rate calculations.

The simplest relationships between sediment solute concentrations and reaction rates occur when solute concentrations in the overlying water are constant and distributions attain a steady-state. Because the overlying water reservoir is generally finite and because many reaction rates, such as organic matter decomposition, change with time, solute concentrations in each reservoir usually cannot attain an exact steady-state. Many simplifying assumptions are commonly appropriate; however, for calculating close approximations to reaction rates from steady-state relationships. When these conditions hold, the experimental method can be quite straightforward.

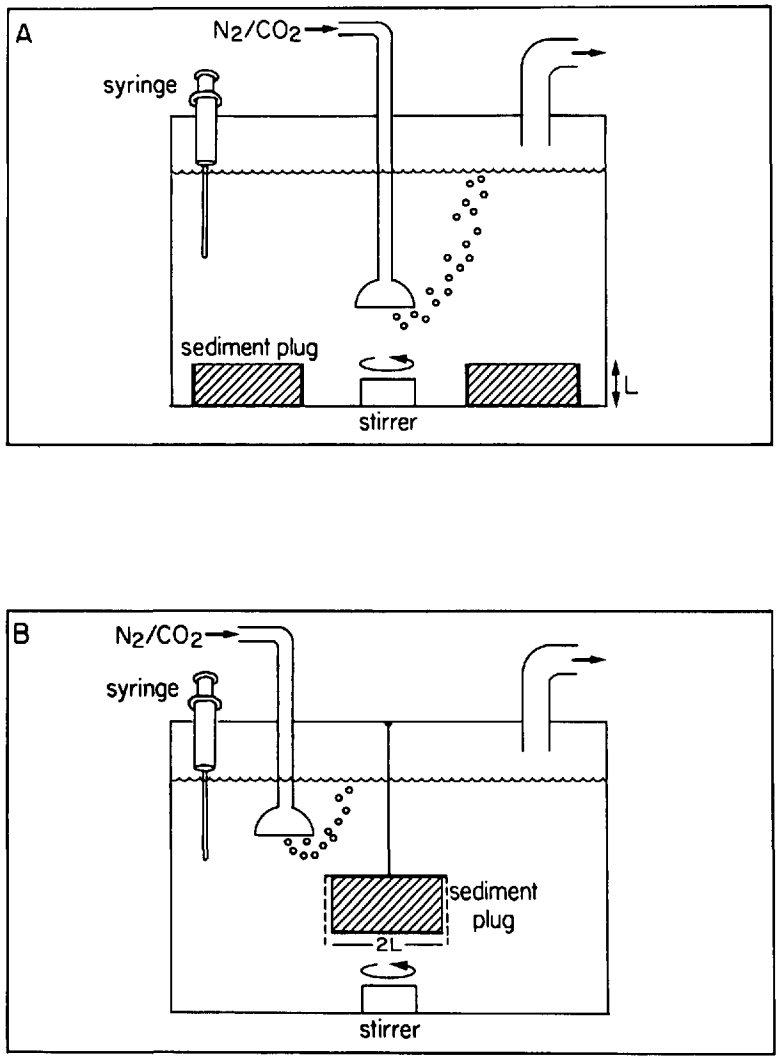

Figure 1. (A) Sketch of typical experimental diffusion reservoir using sediment plugs with one exposed surface. Gas diffusers need not be submerged. (B) Experimental reservoir having plugs with two symmetrically-exposed sides.

The circumstances under which simplifications can be made depend on relative values of reaction rates, plug thickness, exposed sediment area, water reservoir volume, diffusion coefficients, and adsorption properties. The possible behavior of solute concentrations in each reservoir as a function of these variables is developed below and the conditions where steady-state simplifications can be made are outlined.

The distribution of a solute within a stagnant sediment slice represents a balance between diffusive exchange with the contacting well-mixed reservoir and reactions

within the sediment. The concentration, C, of a solute in the sediment pore water is described by:

$$\frac{\partial C}{\partial t} = \frac{D_s}{1 + K}\left(\frac{\partial^2 C}{\partial x^2}\right) + \frac{R}{1 + K} \tag{1}$$

and in the overlying water reservoir, C_T, by:

$$H\left(\frac{\partial C_T}{\partial t}\right) = \phi D_s\left(\frac{\partial C}{\partial x}\right)_{x=0} \tag{2}$$

where:

x = space coordinate, origin at sediment-water interface, positive into the sediment
t = time
D_s = whole sediment diffusion coefficient
K = linear adsorption constant
R = reaction function
ϕ = sediment porosity
A_s = exposed area of sediment plug
V_w = volume of overlying water reservoir
$H = V_w/A_s$.

Two practically useful end-member reaction functions are considered here: a concentration-dependent or first-order reaction term $R = k(C - Ceq)$, and a concentration-independent or zero-order reaction term $R = R_1$; where k = first-order rate constant, Ceq = apparent equilibrium saturation concentration, R_1 = constant. Simple linear, reversible adsorption is also included (Berner, 1976).

The initial and boundary conditions are:

$$\text{Sediment: } t = 0; \quad C = C_o, \qquad 0 \le x \le L \tag{3a}$$

$$t > 0; \quad C = C_T, \qquad x = 0 \tag{3b}$$

$$\partial C/\partial x = 0, \quad x = L \tag{3c}$$

$$\text{Overlying Water: } t = 0;\ C = C_{To} \quad (t > 0;\ C = C_T). \tag{3d}$$

These conditions require spatially constant initial concentrations in both the sediment and water, a well-stirred overlying water reservoir, and that the plug of sediment with sealed sides also has an impermeable lower boundary. Identical equations apply when a sediment slice of thickness $2L$ is used, having both ends freely exposed at $x = 0$ and $x = 2L$ (Fig. 1B). The exact initial distribution in the sediment is not generally critical unless L is large and nonsteady-state behavior at small t is of interest. In order to allow general comparison of the controlling factors, dimensionless variables are introduced.

For the case where $R = R_1$ (zero order), the dimensionless variables used are:

$C^* = C/C_o$	pore water	(4a)
$C_T^* = C_T/C_o$	overlying water	(4b)
$x^* = x/L$	spatial scale	(4c)
$V^* = \phi L(1 + K)/H$	sediment/overlying water reservoir volume ratio	(4d)
$t^* = tD_s/(L^2(1 + K))$	time	(4e)
$R_1^* = R_1L^2/(D_sC_o)$	reaction	(4f)

For the case where $R = k(C - Ceq)$ (first-order reaction with saturation), the dimensionless variables used are:

$C^* = C/Ceq$	pore water	(5a)
$C_T^* = C_T/Ceq$	overlying water	(5b)
$C_o^* = C_o/Ceq$	initial value	(5c)
$k^* = kL^2/D_s$	reaction constant (a Damkholer number)	(5d)

with x^*, t^*, and V^* as before (Eqs. 4c, d, e).

The solutions to the nondimensional forms of Eqs. (1) and (2) with transformed conditions (3) are given in Appendix I.

When the overlying water reservoir is sufficiently large ($V^* \rightarrow 0$) or when t^* is small, then C_T^* can often be assumed constant, or effectively constant. Under these conditions (examined below) only Eq. (1) is applicable with the initial and boundary values (dimensional):

$$t = 0; \quad C = C_o, \quad 0 \le x \le L \tag{6a}$$

$$t > 0; \quad C = C_{To}, \quad x = 0 \tag{6b}$$

$$\partial C/\partial x = 0, \quad x = \mathrm{L} \tag{6c}$$

The appropriate nondimensional solutions for the case of an infinite overlying reservoir (conditions (6)) are also given in Appendix I. The behavior of the models for the two reaction functions and different boundary conditions are now considered separately.

i. Concentration-independent reactions. A steady-state, or a close approximation to a steady-state pore water distribution, can be attained in sediment sections only when C_T^* is constant or effectively constant relative to C^* (condition 6b). The relationships in this case are particularly simple and practically useful, and the circumstances when they are valid are therefore emphasized here.

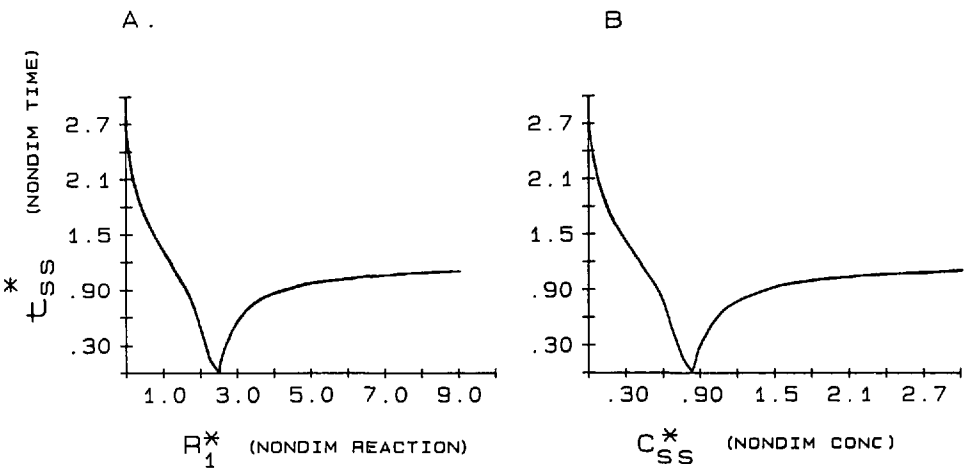

Figure 2. (A) Relation of dimensionless 'time' to steady-state, t^*_{ss}, to dimensionless 'reaction rate', R^*_1, in the infinite reservoir case (C^*_T = constant = 0.01). (B) Relation of dimensionless 'time' to steady-state, t^*_{ss}, to dimensionless steady-state average pore water 'concentration' $\bar{C}^*_{ss}$. Because $\bar{C}^*_{ss}$ in this case is simply proportional to R^*_1, the plot is equivalent to 2A. This illustrates that a minimum ($\neq 0$) occurs when the starting concentration is close to the steady-state value. $t^* \sim 1.2$ represents a case where steady-state is achieved over a wide range of reaction rates (R^*_1).

When C^*_T is constant at the initial value C^*_{To}, and if $\bar{C}^*$ is the dimensionless average concentration in the sediment from $0 \leq x^* \leq 1$ ($0 \leq x \leq L$), then the reaction rate variables are related to the average plug concentration, $\bar{C}^*_{ss}$, at steady-state by:

$$R^*_1 = 3(\bar{C}^*_{ss} - C^*_{To}). \tag{7}$$

Defining the dimensionless time to steady-state, t^*_{ss}, as the time where the averaged concentration in the sediment is within ±5% of the steady-state value, $\bar{C}^*_{ss}$, then roughly:

$$t^*_{ss} \sim \frac{4}{\pi} \ln \left| \frac{0.025\, \bar{C}^*_{ss}(\pi/2)^4}{R^*_1 + (\pi/2)^2(C^*_{To} - 1)} \right|. \tag{8}$$

The exact graphic relationships show that a minimum time occurs at $\bar{C}^*_{ss} \sim 1$, that is, where $\bar{C}_{ss} \sim C_o$ in dimensional variables (Fig. 2). In general, at constant $C^*_T = C^*_{To}$ for a wide range of fixed reaction rates $R^*_1 > 1$, a solute would achieve steady-state in dimensionless time values of $t^* < 1.2$.

The relationships between t_{ss}, R_1, and L in dimensional variables for the general model values in Table 1 when C^*_T is constant at C^*_{To} are shown in Figure 3. These values were chosen as representative of ammonification rates (NH_4^+ production) in nearshore muds. The location of the minimum t_{ss} at a given R_1 and L depends largely on the value of C_o. When reaction rates are low, times of a week or more may be required to achieve

Table 1. Dimensional model values.

Constant reaction		First-order reaction	
Variable	Value	Variable	Value
D_s	1.11 cm²/d	D_s	0.595
ϕ	0.83	ϕ	0.83
K	1.3	K	0
C_{To}	1 μM	k	—
C_o	100 μM	C_{To}	10 μM
R_1	—	C_o	600 μM
L	—	Ceq	800 μM
		L	—

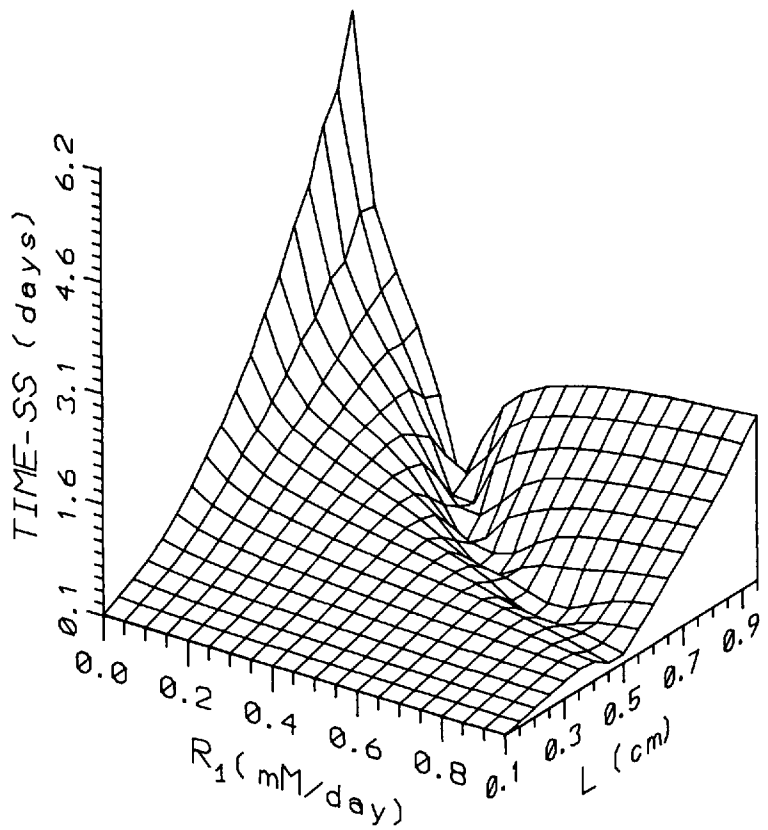

Figure 3. The relation between the dimensional time to steady-state (days) for a representative range of reaction rates (μM/d) and sediment plug thickness (cm) (other model variables as in Table 1).

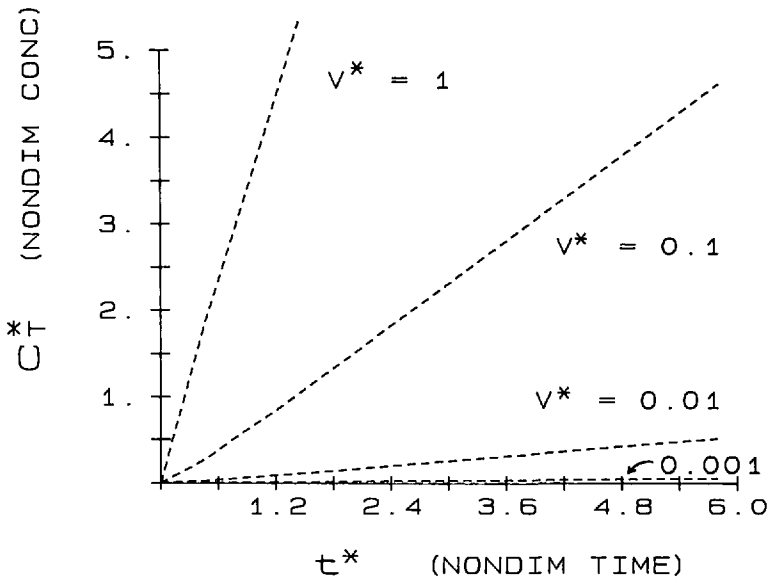

Figure 4. Dependence of dimensionless overlying reservoir concentration. C_T^*, for fixed $R_\uparrow^* = 9.0$ as a function of t^* and V^*. The value of $R_\uparrow^*$ corresponds, for example, to $R_\uparrow \sim 1000\ \mu M/d$ and $L = 1$ with model values of Table 1.

steady-state for $L \geq 1$ cm. Time-dependent solutions can be used if a large L is experimentally desirable. If an approximate value of $R_\uparrow$ is known *a priori,* factors such as L can, in principle, be manipulated to achieve rapid steady-state.

The conditions under which the constant $C_T^* = C_{To}^*$ model is applicable can be investigated by comparison to the more exact finite volume model (conditions 3), under a range of circumstances. The dependence of C_T^* on t^* for various values of V^* and fixed $R_\uparrow^*$ is illustrated in Figure 4 (values of D_s, ϕ, K, C_T, and C_o as in Table 1). The value of $R_\uparrow^* = 9.0$ used in calculations corresponds, for example, to $R_\uparrow = 1000\ \mu M/d$ with $L = 1$ cm ($\mu M = \mu$moles/liter pore water). When V^* is <0.1, C_T^* is not a particularly strong function of t^* for this reaction rate. The dependence of C_T^* on t^* becomes stronger as $R_\uparrow^*$ increases (Fig. 5).

Even when C_T^* is moderately variable, a good approximation to $R_\uparrow^*$ can often be calculated from experimental data using a form of Eq. (7). Figure 6 shows the error incurred in estimating $R_\uparrow^*$ from the steady-state relation (7) at $t^* = 1.2$ and different V^* for various choices of effectively 'constant' C_T^*. The curves shown are for choices of C_{To}^* as the average value of C_T^* over the experiment or as the value of C_T^* at the time of final sampling ($t^* = 1.2$). The 'constant' C_T^* approximation (Eq. 7) is usually valid (error < 10%) for $V^* < 0.1$ and $R_\uparrow^* > 1$ at $t^* \sim 1$, with only moderate error (±20%) over a wide range of conditions (Fig. 6). This error increases as t^* becomes very large, in which case the pseudo steady-state relation outlined below must be used.

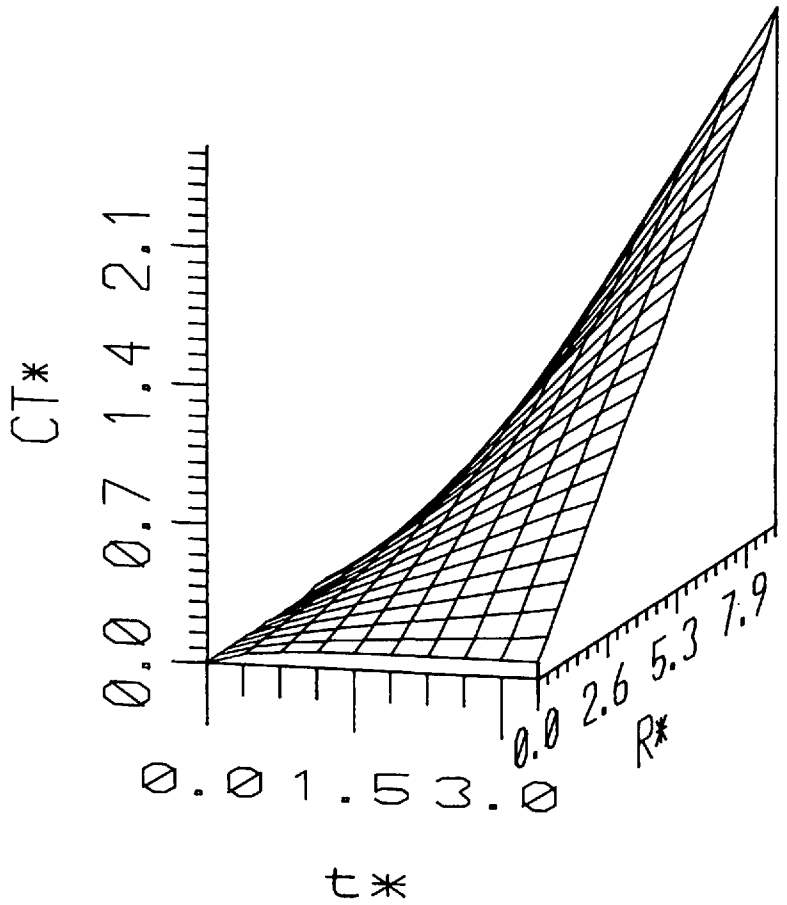

Figure 5. Variation of C_T^* with t^* and $R_\uparrow^*$ when $V^* = 0.5$.

When C_T^* varies significantly relative to $\bar{C}^*$ the simple relation (7) is no longer even approximately valid and the exact finite reservoir model with condition 3 must be used. Regardless of time variation in the overlying water solute concentration, a pseudo-steady-state relation does occur where the *difference*, $(\bar{C}^*(t^*) - C_T^*(t^*))$, between the individually time-dependent average reservoir concentrations, $\bar{C}^*(t^*)$ and $C_T^*(t^*)$, becomes constant. This pseudo-steady-state ($\bar{C}^* - C_T^*$ = constant) is also achieved when $t^* > 1.2$ for a large range of $R_\uparrow^*$. The pseudo-steady-state value of $\bar{C}^* - C_T^*$ when C_T^* is not constant is given by (see Appendix I for definitions):

$$\bar{C}^* - C_T^* = (C_{To}^* + V^* - R_\uparrow^*/6)/(1 + V^*) + R_\uparrow^*(1 + V^*/3)/(2(1 + V^*)2) - C_{To}^* - V^* \sum_{n=1}^{\infty} \left[\frac{(R_\uparrow^* + \alpha_n^2(C_{To}^* - 1) \sin(\alpha_n)}{\alpha_n^3 \Delta_n^*} \right]. \quad (9)$$

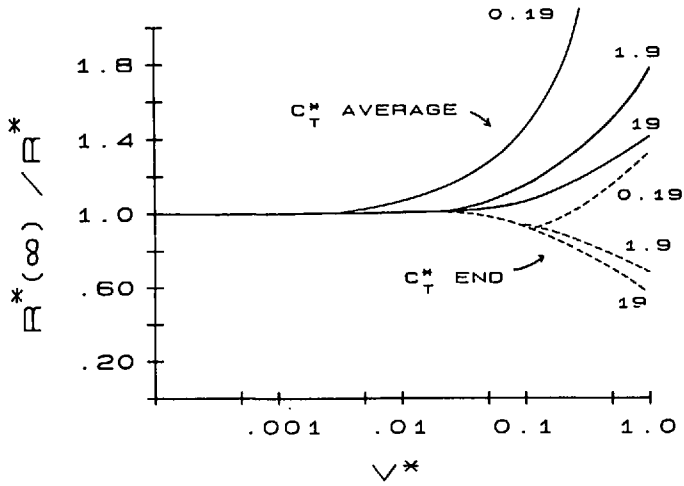

Figure 6. Even when C_T^* actually varies, the simple 'constant' C_T model may still give acceptable estimates of $R_\uparrow^*$ under many conditions. In this case, the ratios of reaction rate estimates, $R_\uparrow^*$, made from the finite reservoir model Eq. (7) and labeled $R_\uparrow^*(\infty)$, are compared to the exact finite reservoir value of $R_\uparrow^*$, for different V^* and ranges of $R_\uparrow^*$. The time of the estimates in these cases is $t^* = 1.2$. Two types of approximations to a 'constant' $C_{T_o}^*$ are made. For the set of solid curves, the average value of a measured range of C_T^* up to $t^* = 1.2$ is used as an experimentally 'constant' C_T^* in Eq. 7. The dashed curves use only the value of $C_{T_o}^* = C_T^*$ at the time ($t^* = 1.2$) at which $\bar{C}^*$ is measured (end of experiment). The numbers on each curve indicate the actual value of $R_\uparrow^*$ as determined from $\bar{C}^*$ using the finite reservoir calculation. Eq. 7 generally gives a good approximate to $R_\uparrow^*$ (from a given value of $\bar{C}^*$) for $V^* < 0.1$ and $R_\uparrow^* > 1$ at $t^* = 1.2$. The approximation becomes worse as V^* becomes large and C_T^* varies greatly with t^*.

If no reactions occur in the overlying water, the steady-state or pseudo-steady-state flux of a solute from the plug into the overlying water gives an additional measure of the zeroth-order reaction rate. The dimensional form of the solute flux from or into the sediment plug is:

$$J = -\phi D_s \left(\frac{\partial C}{\partial x}\right)_{x=0} \tag{10}$$

and the nondimensional flux J^* is:

$$J^* = \frac{JL}{\phi D_s C_o} = -\left(\frac{\partial C^*}{\partial x^*}\right)_{x^*=0}. \tag{11}$$

For values of $t^* > 1$ the flux into a finite or infinite ($V^* = 0$, $C_T^* =$ constant) reservoir becomes:

$$J^* = -R_\uparrow^*/(1 + V^*). \tag{12}$$

In the case of a concentration-independent reaction, the flux from the sediment is not time-dependent after initial conditions are no longer of influence.

One advantage to minimizing changes in C_T^* is inhibition of possible secondary reactions in the water reservoir. A second advantage is that $\bar{C}^*$ is minimized for a given reaction rate so that tests of assumed kinetic relations are best made with $C_T^* \sim$ constant. The pseudo-steady-state relation given by Eq. (9) or the exact time-dependent solutions can always be used to calculate R_1^* when C_T^* varies significantly or at small t^* (exact solution).

ii. Concentration-dependent, first-order reactions. When the water reservoir is sufficiently large so that C_T^* is effectively constant or equivalently $V^* \rightarrow 0$, then a steady-state distribution is also attained for solutes subject to first-order reaction rates. The average concentration in the sediment at steady-state is given by:

$$\bar{C}_{ss}^* = 1 + \frac{(C_{To}^* - 1) \tanh \sqrt{k^*}}{\sqrt{k^*}}. \tag{13}$$

The approximate time to steady-state, t_{ss}^*, (95% of steady-state) in a sediment plug for first-order reactions is:

$$t_{ss}^* \sim -\frac{1}{\beta} \ln \left| \frac{0.025\,(\bar{C}_{ss}^* \beta \pi^2/4)}{C_{To}^* \pi^2/4 + k^* - C_o^* \beta} \right| \tag{14a}$$

where,

$$\beta = k^* + \pi^2/4. \tag{14b}$$

In the case of solutes subject to first order reactions, the pseudo-steady-state relation where $(\bar{C}^*(t^*) - C_T^*(t^*)) =$ constant (Eq. 9), is not possible. Characteristic variation of t_{ss}^* for different initial conditions and k^*, demonstrate that for many practical ranges of variables $t_{ss}^* < 2$ and often $t_{ss}^* < 1$ (Fig. 7). Minimum times occur when initial conditions are close to those dictated by a steady state ($C_o^* \sim \bar{C}_{ss}^*$). When a steady-state does occur, the reaction rate variables are related to the mean solute concentration in the sediment section by:

$$\sqrt{k^*} \coth \sqrt{k^*} = (C_T^* - 1)/(\bar{C}_{ss}^* - 1) \tag{15}$$

For $k^* > 1$, $\coth \sqrt{k^*} \sim 1$ so that Eq. (15) can often be further simplified.

Assuming that an experimental set-up were sampled at $t^* = 1.2$ (sufficient for near steady-state in many cases when $C_T^* \sim$ constant), then the error in calculating k^* from $\bar{C}^*$ using an infinite reservoir ($V^* = 0$) compared to an exact finite reservoir model ($V^* > 0$) depends on V^* and the choice of the effective value of C_{To}^* used in calculations (Fig. 8). For many practical cases where $V^* < 0.1$, an error of <20% in calculating k^* occurs when either the average value of C_T^* over the time of the experiment or the value

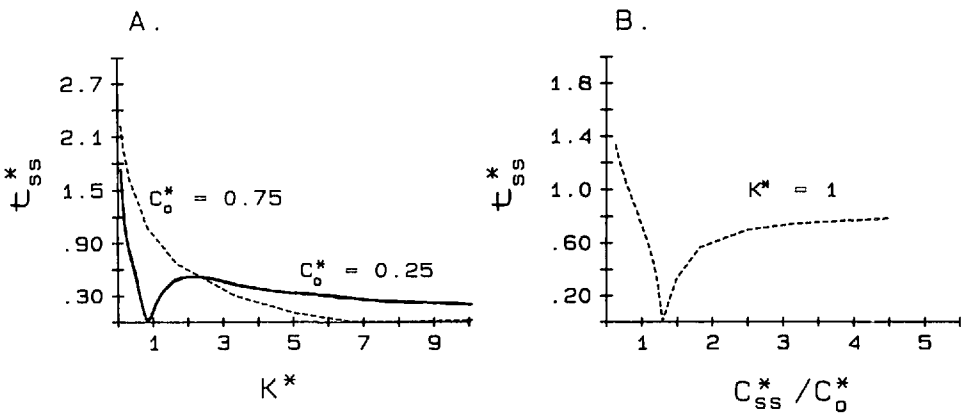

Figure 7. (A) Examples of the dependence of dimensionless 'time' to steady-state, t^*_{ss}, on C^*_o and k^* for first-order reaction at fixed C^*_T (=0.012). (B) A minimum t^*_{ss} ($\neq 0$) occurs when C^*_o is close to steady-state $\bar{C}^*$.

at the time of sampling (t^*) is used for the infinite reservoir approximation (C^*_{To}). As in the zero-order reaction case, the use of a steady-state approximation allows ready estimation of reaction rates using simple equations such as (15). These estimates may be used as starting values in more exact calculations with the finite reservoir model. Large differences between the finite reservoir and the approximate infinite overlying reservoir model estimates can occur as t^* becomes large.

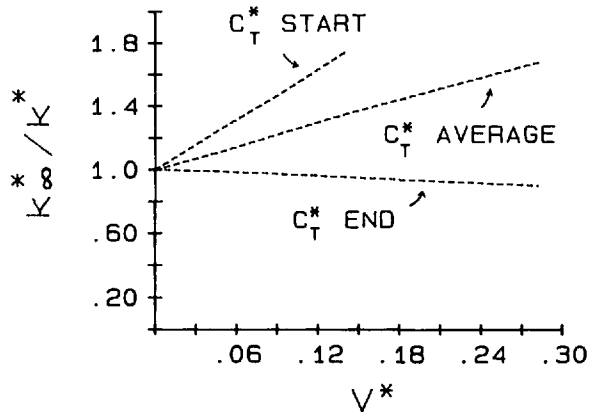

Figure 8. Ratio at $t^* = 1.2$ of k^* calculated from $\bar{C}^*$ using an approximate version of the infinite reservoir model steady-state solution (Eq. 15; indicated as $k^*(\infty)$) compared to an exact calculation of k^* using the finite reservoir model at various effective values of V^*. The curves represent different hypothetical ways of experimentally choosing C^*_{To} used in the infinite volume calculation. Little difference in the models is found when $C^*_{To} = C^*_T$ at time of collection ($t^* = 1.2$) is used in Eq. 15, while the greatest discrepancy occurs when $C^*_{To} = C^*_T(t^* = 0)$ is used in calculation.

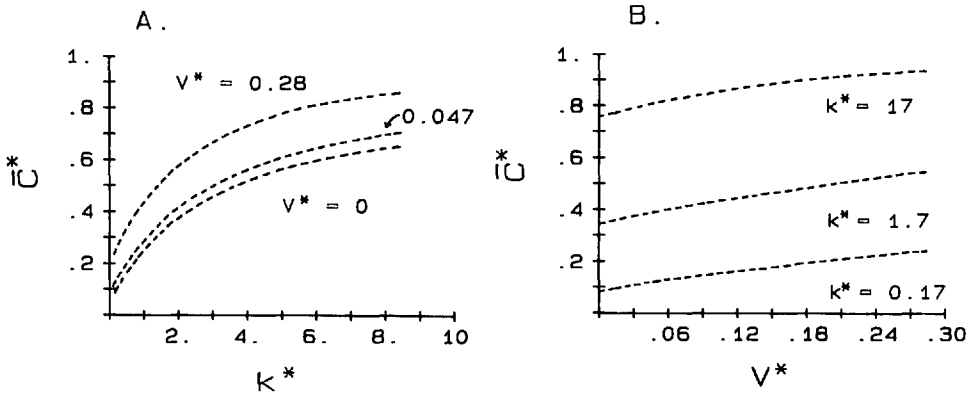

Figure 9. (A) Relation of average $\bar{C}^*$ to k^* at fixed values of V^* when $t^* = 1.2$ ($C^*_{To} = 0.012$). Highest experimental sensitivity ($\partial\bar{C}^*/\partial k^*$) occurs when $k^* < 3$. (B) At a fixed value of k^*, the measured $\bar{C}^*$ ($t^* = 1.2$; $C^*_{To} = 0.012$) varies almost linearly with possible experimental choices of V^* (reservoir volume ratio).

Examples of the predicted behaviors of $\bar{C}^*$ and C^*_T in the finite reservoir case are shown in Figures 9 and 10. The average pore water concentration $\bar{C}^*$ is a sensitive measure of k^* for $k^* < 3$, but experimental uncertainty in estimating k^* from $\bar{C}^*$ increases substantially as k^* becomes large (for a given precision of measuring $\bar{C}^*$). The time-dependence of overlying water reservoir concentration, C^*_T, depends strongly on the value of k^* and choice of V^* (Fig. 10).

The solute flux from the sediment for first-order reaction with saturation is given from Eqs. (10), (11) and the appropriate solutions in Appendix I. For large values of t^* in the finite reservoir case, $J^* = LJ/(\phi D_s Ceq) = 0$, as $C^*_T \rightarrow 1$ (saturation). In the case

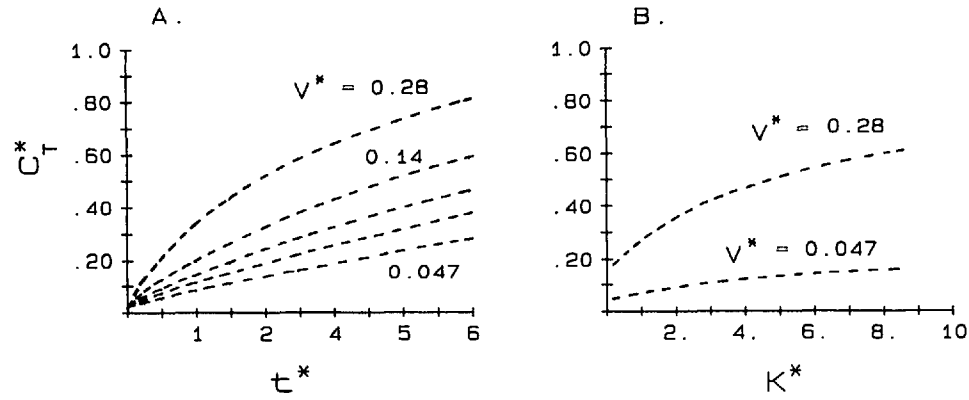

Figure 10. (A) Variation of C^*_T with t^* as function of V^* at $k^* = 1.7$ ($C^*_{To} = 0.012$). (B) Variation of C^*_T with k^* as function of V^* at $t^* = 1.2$.

of the infinite reservoir at steady-state (when $V^* \sim 0$ and $C_T^* \sim C_{To}^*$), then:

$$J^* = -(C_{To}^* - 1)\sqrt{k^*}\tanh\sqrt{k^*}. \tag{16}$$

If a value of *Ceq* is known independently from a separate closed incubation experiment ($V^* \to \infty$ or $t^* \to$ large for V^* small), then Eqs. (15) and (16) allow independent measures of k. Otherwise (15) and (16) can be used together to estimate k and *Ceq* simultaneously by best fit to the flux and concentration data. The relative sensitivity of the different measures, C^* and J^*, for estimating k^* at steady state is illustrated in Figure 11. Both measures lose sensitivity as $C_{To} \to Ceq$ and $k \to$ large. Experimental scaling can be optimized for sensitivity if a general range of reaction constants is known *a priori*.

iii. Two-layer models. In some situations, the sediment used in plug incubations is sufficiently unstable that a thin screen or porous membrane may be necessary to maintain the integrity of the plug. This is particularly true when a two-sided plug is used and the axis of the sediment may be horizontal rather than vertical (Fig. 1B). The solute concentrations in the sediment and sediment-water fluxes are now determined in part by the properties of the retaining cover material. Assuming that no reactions occur in the screen or membrane of thickness L_1, then the concentration distributions in each region are given by:

Layer 1 (cover membrane), $0 \le x \le L_1$

$$\frac{\partial C_1}{\partial t} = D_1 \frac{\partial^2 C_1}{\partial x^2} \tag{17a}$$

Layer 2 (sediment), $L_1 \le x \le L_2$

$$\frac{\partial C_2}{\partial t} = \frac{D_2}{1 + K}\frac{\partial^2 C_2}{\partial x^2} + \frac{R}{1 + k} \tag{17b}$$

Zone 3 (overlying water):

$$H\frac{\partial C_T}{\partial t} = \phi_1 D_1 \left(\frac{\partial C_1}{\partial x}\right)_{x=0}. \tag{17c}$$

Rather than presenting the exact solutions, the steady-state solutions for $C_T =$ constant are used to illustrate solute behavior for various properties of covering membranes (exact time-dependent solutions are readily obtained, e.g. Aller, 1978).

The steady-state, dimensional solutions for $R = R_1$ (a constant); $C_T =$ constant, flux and concentration matches at L_1, and an impermeable lower boundary as before (Eq. 3c) give:

$$\begin{aligned} C_1 &= C_T + \phi_2 R_1 \Delta L x/(\phi_1 D_1) \\ C_2 &= C_T + \phi_2 R_1 L_1 \Delta L/(\phi_1 D_1) + R_1(\Delta L)^2/(2D_2) \\ &\quad - R_1(x - L_2)^2/(2D_2) \end{aligned} \tag{18}$$

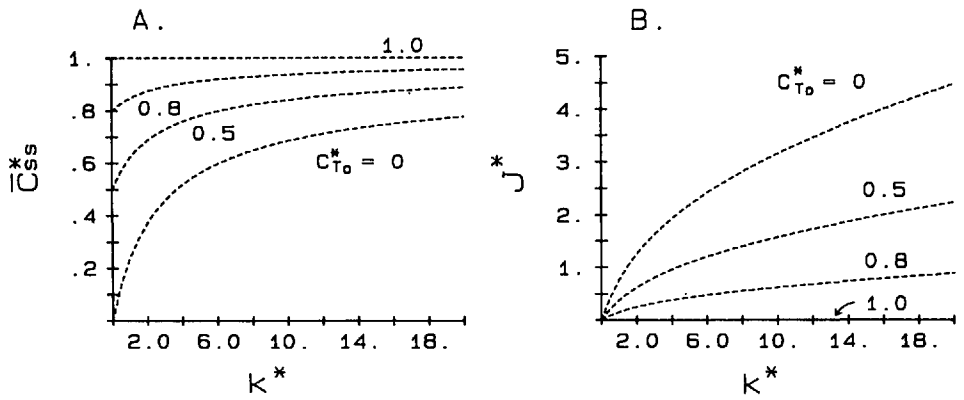

Figure 11. (A) Examples of variation at steady-state of the averaged pore water concentration, $\bar{C}^*_{ss}$ as a function of k^* and C^*_{To} (marked on curves). (B) Variation in J^* at steady-state as a function of k^* and C^*_{To}. The experimental sensitivity of the measures $\bar{C}^*$ and J^* to calculate differences between reaction constants drops at large k or as $C_{To} \rightarrow Ceq$ for a given plug thickness (other model values in Table 1).

where:

$$\Delta L = (L_2 - L_1)$$

and:

$$\bar{C}_{ss} = C_T + R_1\left[\frac{(\Delta L)^2}{3D_2} + \frac{\phi_2 L_1 \Delta L}{\phi_1 D_1}\right] \qquad (19)$$
$$J = -\phi_2 R_1 \Delta L.$$

The steady-state solutions for $R = k(Ceq - C_2)$ in the sediment zone with boundary conditions as before are:

$$C_1 = C_T + A_1 x \qquad (20)$$
$$C_2 = Ceq + A_2 \cosh(\sigma \Delta L)$$

where:

$$\sigma = \sqrt{k/D_2}$$
$$A_1 = -\frac{\phi_2 D_2}{\phi_1 D_1} A_2 \sigma \sinh(\sigma \Delta L)$$
$$A_2 = \frac{(C_T - Ceq)}{\frac{\phi_2 D_2}{\phi_1 D_1} L_1 \sigma \sinh(\sigma \Delta L) + \cosh(\sigma \Delta L)} \qquad (21)$$
$$\bar{C}_{ss} = Ceq + A_2 \sinh(\sigma \Delta L)/(\sigma \Delta L)$$
$$J = \phi_2 D_2 A_2 \sigma \sinh(\sigma \Delta L).$$

Comparison of these solutions with their respective one-layer analogues (Eqs. 7, 12, 13, 16), demonstrates immediately that when $L_1 \ll L_2$ and $\phi_1 D_1 \sim \phi_2 D_2$, there is generally little significant difference between the one and two layer cases. For example, a Nytex screen of 60 μm mesh openings ($\phi_1 = 0.45$, D_1 = free solution value and $L_1 = 55$ μm), would have almost no discernable effect on a sediment plug of 1 cm thickness and only a $\sim 5 - 10\%$ correction would be necessary for a 1 mm thick plug (depending on exact values of ϕ_2, D_1, D_2). The presence of a membrane or stagnant layer can be significant for concentration-dependent reactions when, for example, k is large enough so that $\sqrt{k/D_2}\, L_1 \sim 1$ (Boudreau and Guinasso, 1980; Santschi *et al.*, 1984). Some apparently porous membranes (e.g. paper and glass fiber filters) may be quite tortuous (D_1 very small) so that care must be used in choosing a covering material if one is needed. In general, membrane covers should be avoided to reduce the possibility of unanticipated artifacts, but when required, are unlikely to have experimentally major effects for many solutes over a range of common conditions.

b. Whole-core incubation

A particularly useful variation of these incubation techniques allows L to become large and the overlying reservoir vanishingly small or absent. In this case, the depth dependence of reaction rates usually becomes significant over an undisturbed sediment interval. If a basic mathematical form for a reaction rate is assumed, for example an exponential decrease with depth, and diffusion coefficients are known, then the change in the pore water solute profile with time of incubation allows calculation of the reaction function. The assumption is that solute distributions in incubated sediment intervals can be described by nonsteady-state transport-reaction models. The design of this 'whole-core incubation' provides a relatively labor-free method for determining vertical distributions of reaction rates such as solute release during organic matter decomposition. Because whole cores of sediment are incubated, time-consuming manipulation and incubation of numerous discrete intervals are avoided.

Typically, two or more cores of sediment are removed from a site and one core is sectioned and sampled immediately for initial pore water solute profiles. Other cores are sealed at both ends with a gas-impermeable material (e.g., Saran wrap) without significant overlying water or air spaces. These cores are incubated for appropriate time periods and then sectioned and sampled for pore water solute profiles which have grown-in over time. Use of 'whole core' squeezing techniques may further simplify the procedure (Jahnke, 1988).

Solute distributions in incubated whole cores are affected by boundary and initial conditions that differ somewhat from those previously used with Eq. (1). These are:

Initial condition:

$$C = a + bx + dx^2 + ex^3 + fx^4. \tag{22a}$$

Boundary conditions:

$$x = 0, x = L; \qquad \partial C/\partial x = 0 \tag{22b}$$

where L is the core length and other parameters are defined previously. The initial condition given here is a polynomial with constants a, b, d, e, and f, sufficiently general to give a description of most solute profiles determined in the first core sampled. Boundary conditions reflect the presence of impermeable caps at *both* ends of the incubated cores.

The reaction rates for solutes that are mainly affected by organic matter decomposition in surface (0–20 cm) sediments often are zeroth-order with respect to their own concentration and have the form of $R = R_o e^{-\alpha x} + R_1$, where R_o, α, and R_1 are constants. A straightforward numerical scheme is used with this general reaction function, modified to include adsorption, boundary and initial conditions (22) and Eq. (1); to predict solute distributions as a function of time in incubated whole cores (Appendix II).

i. Model predictions. The integrated reaction rate or flux $(R_o(1 - e^{-\alpha L})/\alpha + R_1 L)$ within the enclosed cores can be determined simply from the adsorption corrected average concentration differences between incubated and initial cores. In this instance, the technique is the same as nondiffusion incubation methods and the profile structure is not used. Values of R_o, α, and R_1 can be determined explicitly by best-fit variation of solutions of Eq. (1) to profiles from incubated cores.

When total reaction rates are high relative to initial concentrations, solute distributions in incubated cores are strongly dependent on reaction parameters in a short time and this remains true for longer periods (Fig. 12; $L = 15$ cm in this case, other variables in Table 1). Low reaction rates require long incubation times for solute distributions to become sensitive to the attenuation of reaction rates with depth (Fig. 13). Therefore, when an *a priori* estimate of total reaction fluxes cannot be made for a particular environment, a relatively long incubation time (10–20 days in nearshore sediments) is recommended. Figures 12 and 13 show that solute distributions near the surface of cores are particularly sensitive to values of reaction parameters. For this reason, cores should be sampled at fine intervals (e.g., 1 cm) near the surface, whereas only coarse sampling intervals are required near the base.

3. Examples of application

Reaction rates estimated from estuarine surface sediments in Mud Bay, South Carolina are used to illustrate some aspects of the plug incubation method (see Aller, 1980; Ullman and Aller, 1980; Mackin and Aller, 1984; for collection-site description; Station 5). In the first example, cores collected (Sept. 1981) by divers were sectioned into discrete 1 to 2 cm depth-intervals. All sediment manipulation and experimental set-up was done in an N_2-filled glove bag. Sediment intervals were individually

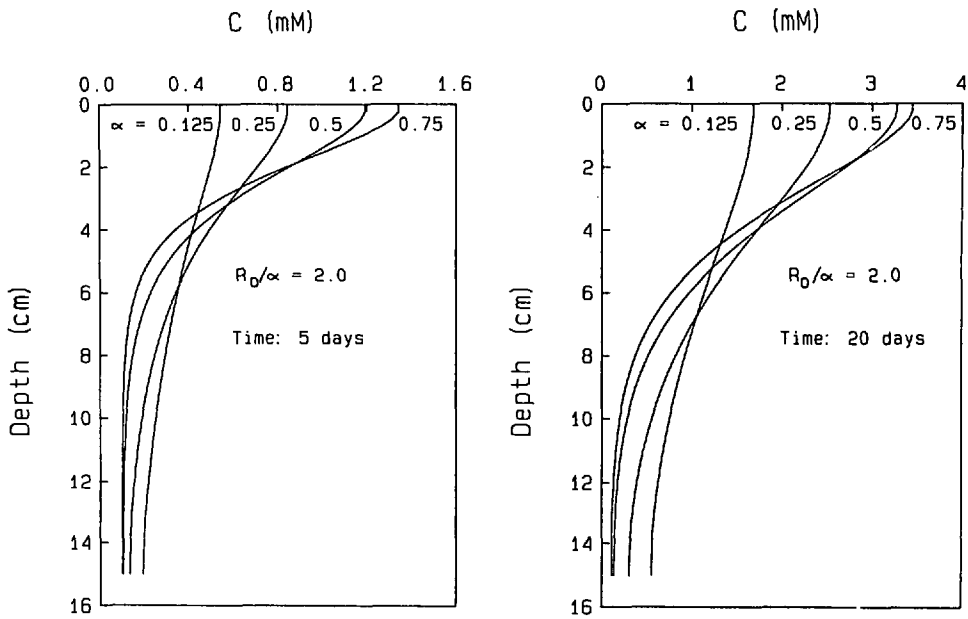

Figure 12. Predicted solute distributions after 5 and 20 days of whole-core incubation, using a constant C_o = 100 μM initial concentration for illustration (other parameters in Table 1 or in the text). For these plots, the total reaction flux ($\sim R_o/\alpha$) was held constant and R_o (mM/day) and α were varied. The total reaction flux in this case (2 μmol/cm^2/day) represents a likely upper bound for NH_4^+ in nearshore sediments.

homogenized by hand and then divided into portions used for closed and open incubations. No water was added to the natural sediment.

For the closed incubation, sediment from each interval was packed into a series of centrifuge tubes, sealed, and stored under N_2. Individual tubes were sampled successively to produce a time-series of concentration change (see, for example, Martens and Berner, 1974; Aller and Yingst, 1980; Ullman and Aller, 1983; Crill and Martens, 1987). The rate of change of concentration of a solute, corrected for adsorption, was used as an estimate of reaction rate. In the case of $Si(OH)_4$, the asymptotic concentration reached after a short period (9 days) was also used to estimate an apparent saturation value, *Ceq*, assuming first-order reaction kinetics apply for Si (Hurd, 1972; Schink *et al.*, 1975). All incubations were done at 26°C.

A set-up similar to Figure 1A was used in open incubations. Sediment was packed into lexan plugs of 1 or 2 cm thickness, having one open end. The sediment in this case was covered by a thin layer of nylon screen (Nytex 44 μm mesh). Plugs were placed into one liter bottles of N_2-purged and filtered sea water and incubated in the dark at 26°C. Water samples were taken periodically. After ~8 days, sediment plugs were sampled for pore waters. Starting pore water solute concentrations, C_o, were taken to be the same as the initial values from closed incubations.

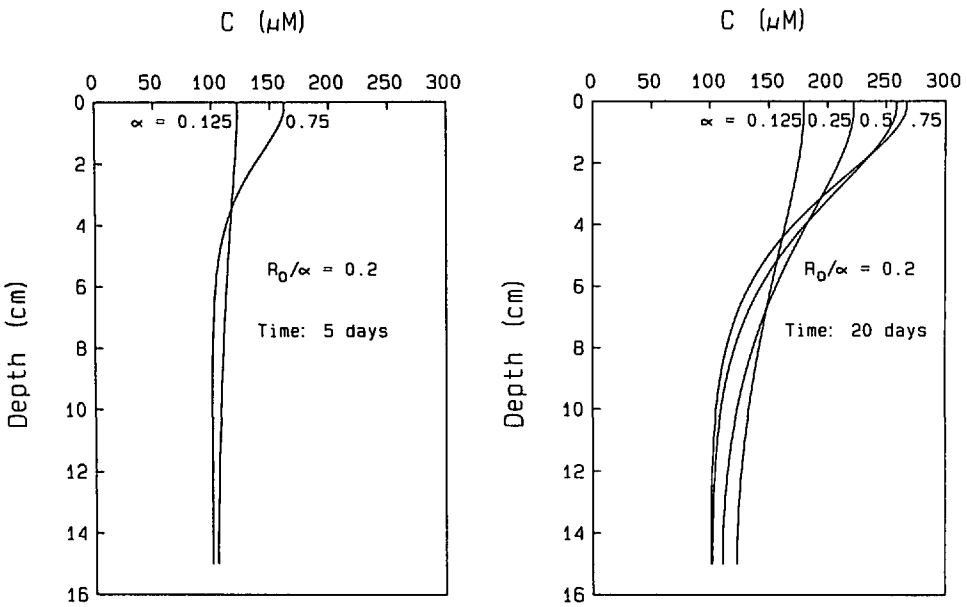

Figure 13. Predicted solute distributions after 5 and 20 days of whole-core incubation using a constant C_o = 100 μM initial concentration (see Fig. 12; R_o in μM/day in this case). The total reaction flux (0.1 μmol/cm²/day is a reasonable lower bound for NH_4^+ in nearshore sediments.

Estimates of NH_4^+, I^-, and $HPO_4^=$ production were made assuming zero-order kinetics. Adsorption coefficients of 0.9–1.3, 0, and 1.9 were used for NH_4^+, I^-, and $HPO_4^=$ respectively (Mackin and Aller, 1984; Krom and Berner, 1980). Variation in adsorption coefficients for NH_4^+ reflects porosity differences in surface versus deeper sediment; insufficient knowledge of $HPO_4^=$ adsorption prevents equivalent corrections. Diffusion coefficients were estimated from the relation $D_s \sim \phi^2 D_o$, where D_o is the appropriate free solution diffusion coefficient (Li and Gregory, 1974; Ullman and Aller, 1982). Both the finite reservoir and the infinite reservoir steady-state models were used to estimate production rates from average pore water concentrations.

Except for the closed $HPO_4^=$ incubation estimate, all methods show fairly good agreement (±20%) and demonstrate the expected overall decrease of rates with depth (Figs. 14, 15). The flux-based estimates agree reasonably well with those calculated from pore water concentrations of I^- and $HPO_4^=$ (Figs. 14, 15). No substantial increase in NH_4^+ was observed in the overlying water reservoirs. Nonexclusive reasons may be that NH_3 was stripped from overlying water at the slightly elevated pH (~9) caused by N_2 bubbling, consumed by bacterial growth, or lost by microaerophilic oxidation to NO_3^- (followed by denitrification) due to any small O_2 contamination. The former problem can be eliminated by use of N_2/CO_2 mixtures or use of an anaerobic incubator. Multiple plugs from a given interval are also advisable to increase measurement precision.

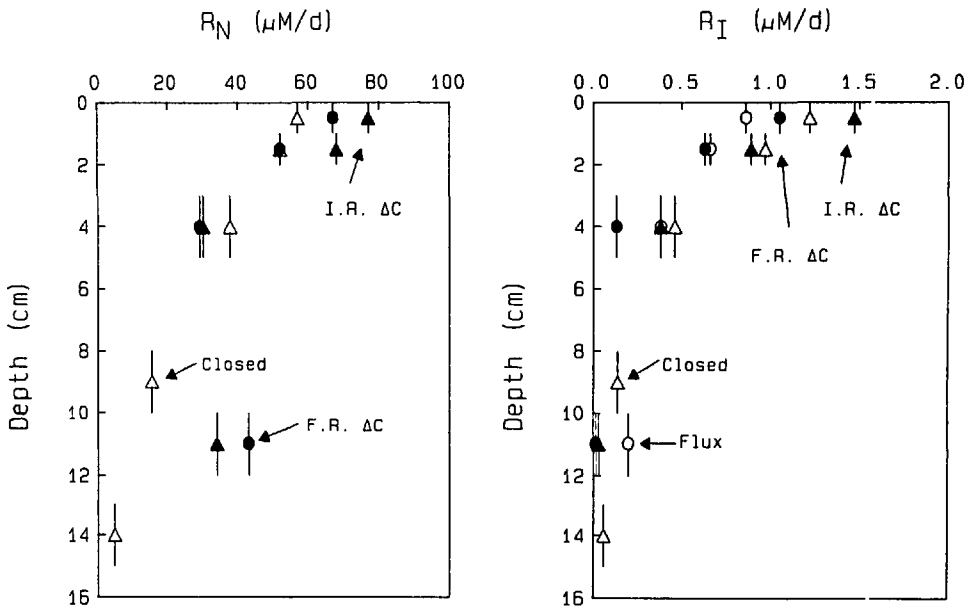

Figure 14. Measured production rates of dissolved iodine and ammonium as function of depth in Mud Bay, SC sediment. Estimates were made using rates of concentration increase in closed incubations (closed), flux from sediment plugs (finite reservoir model = FLUX), average concentration in pore water assuming a finite reservoir model with variable C_T (F.R. ΔC), and average pore water concentration assuming an infinite reservoir at steady-state (Eq. 7) with a fixed C_{To} taken as the mean value of C_T over the time of experiment (I.R. ΔC) (T = 26°C).

Subsequent experiments have shown that net release rates of constituents like NH_4^+ may not be zero-order over the entire concentration range (Aller and Aller, in preparation), but for the ranges in the present experiments, closed and open incubations agree well. Comparisons of this type can be used to check assumptions regarding reaction kinetics. A major advantage of the open incubation method is that, near steady-state, the value of K, the adsorption coefficient, does not influence rate estimates (Berner, 1976). A disadvantage is that diffusion coefficients must be known except in the case of zero-order reactions. Measurement of sediment resistivity or porosity provides a basis for estimating diffusion coefficients if free solution values are known (Andrews and Bennett, 1981; McDuff and Ellis, 1979).

Effective first-order reaction constants for $Si(OH)_4$ were also estimated from the closed and open incubations described previously. The values of *Ceq* used in calculations for the plugs were obtained from stable values attained in the corresponding closed incubations (Fig. 16). These experiments demonstrate a general decrease in the mean effective k with depth, when estimates of k from pore water concentrations and flux-derived calculations are combined.

The plug-incubation method can be used to examine the interdependence of classes

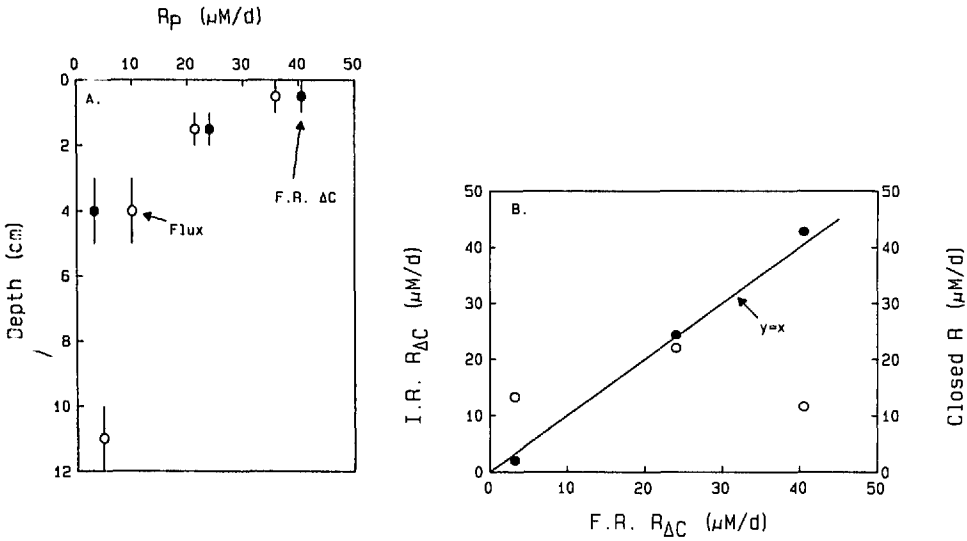

Figure 15. (A) Mud Bay $HPO_4^=$ production rates estimated from flux and pore water concentrations (F.R. ΔC) using the finite reservoir model. (B) Relation of infinite and finite reservoir production estimates using pore water concentrations (●); a good correspondence is found. The closed incubation estimates (o) do not agree well with diffusion plugs, probably due to inaccurate estimates of adsorption coefficients which may vary with depth. (T = 26°C).

of reactions. For example, one pathway of Mn-reduction is by reaction with dissolved HS^- produced during SO_4-reduction (Burdige and Nealson, 1986). At least a partial separation of Mn-reduction by organic C, as opposed to dissolved HS^-, can be made by open incubation of sediment in SO_4-free overlying water. In the present case, undisturbed (unmixed) plugs of sediment from different depth intervals in Mud Bay, South Carolina (March, 1981) were placed in N_2-purged 0.4 M NaCl. A set-up similar to Figure 1B was used with Whatman #1 filters covering the ends of the plugs (these cellulose-based filters are no longer used in experiments because of relatively high diffusive tortuosity of filter material and possible bacterial decomposition of the filters). Eq. 8 was used to convert measured Mn^{++} fluxes out of the plugs at near steady-state into estimates of reaction rates as a function of depth (T = 12°C) (Fig. 17). Calculations show that $SO_4^=$ was <0.08 mM in these plugs after several hours, implying that reduction of Mn^{++} at the observed rates was very unlikely to be caused by dissolved HS^- produced by active $SO_4^=$ reduction. This does not preclude Mn-reduction by solid phase sulfide oxidation (Aller and Rude, 1988). The main point is that the open-incubation method allows manipulation of pore solution composition by varying overlying water boundary conditions as well as plug thicknesses. These manipulations can be used to examine mechanisms of reactions.

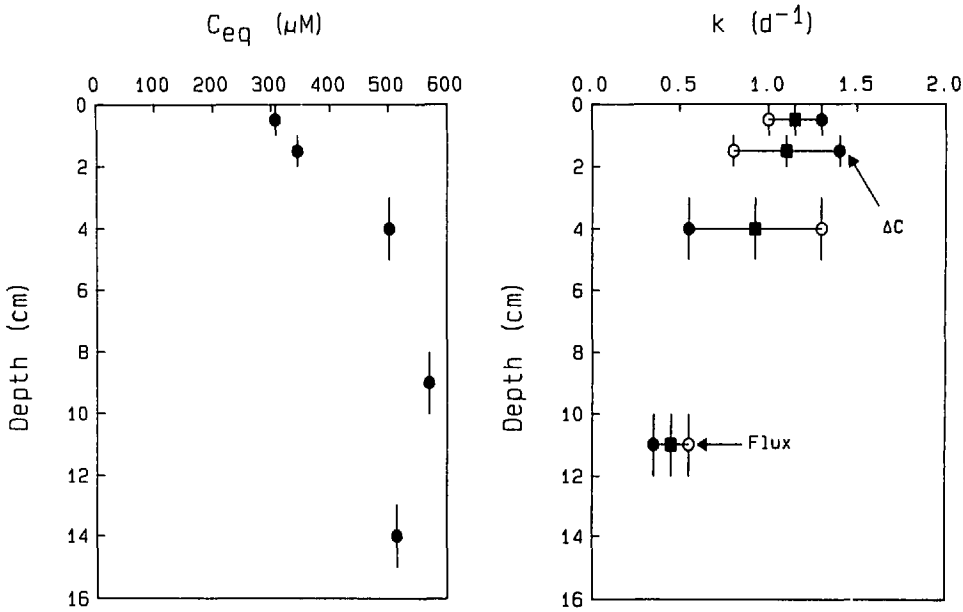

Figure 16. Estimates of *Ceq* (closed incubations) and *k* (diffusion plugs) as function of depth in Mud Bay, SC sediments. The mean value of *k* estimated from pore water and fluxes (finite reservoir model) decreases with depth. *Ceq* is lower in the surface few centimeters where Fe, Mn-oxides are present than in deeper sediment. (T = 26°C).

The whole-core incubation technique was tested with sediment collected using a box corer at a mud site in western Long Island Sound near Greenwich, Connecticut (Aug. 1987). One core (acrylic liner, 165 cm^2 cross-sectional area) was removed from the box core and sectioned for closed-incubation experiments as described earlier. Two subcores of 7.6 cm O.D., 0.3 cm wall thickness were removed for whole-core incubations. One of these cores was sampled immediately for pore waters. The ends of the other core were covered with Saran wrap (O_2 impermeable) and capped (core caps held with hose clamps). The core was incubated in the dark at the *in situ* temperature (22 ± 0.5°C) for ~12 days and sectioned and sampled for pore waters. Sediment manipulations and sampling were performed under N2.

Figure 18 shows dissolved NH_4^+, $SO_4^=$ and alkalinity as a function of depth and time in the whole-core incubation experiment. Numerical best-fits of Eq. (1) to the incubated core data were determined using solute free-solution diffusion coefficients corrected for tortuosity, as discussed previously (ϕ = average porosity in the core), polynomial best-fits to the initial core data (Fig. 18) and assuming K = 1.3 for NH_4^+ and K = 0 for $SO_4^=$ and alkalinity. Alkalinity is almost entirely HCO_3^- at the pH of these sediments (pH = 7.4 ± 0.1).

The rate functions necessary to fit the whole-core incubation profile data are compared to rates determined from closed incubations of discrete intervals in

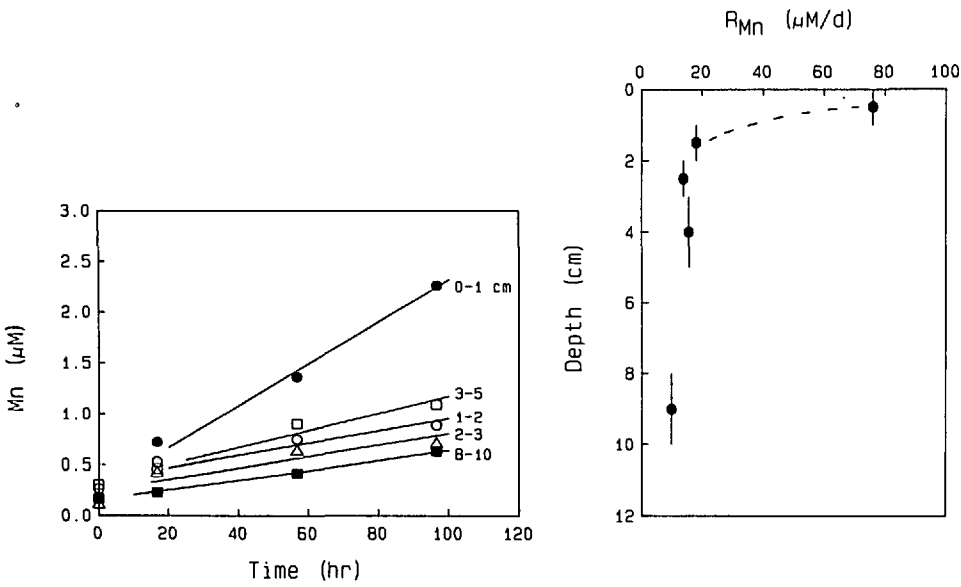

Figure 17. (A) Mn^{++} concentration in overlying water reservoir as a function of time in SO_4-free, anoxic plug experiment. (B) Calculated production rate of Mn^{++} as function of depth in Mud Bay sediments using the infinite reservoir approximation (T = 12°C).

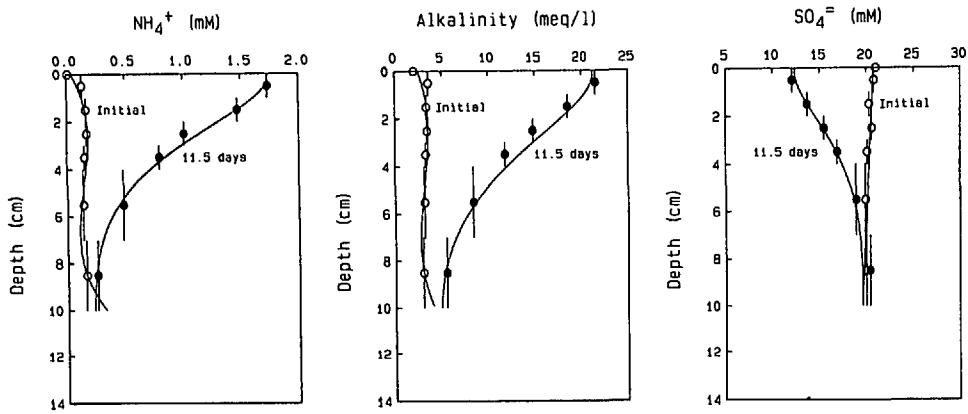

Figure 18. Comparisons of initial (time of collection) solute profiles in a core from Long Island Sound and corresponding profiles following 11.5 days of whole core incubation. The differences in profiles are used to calculate the rate functions in Figure 19, using the whole core incubation calculation method.

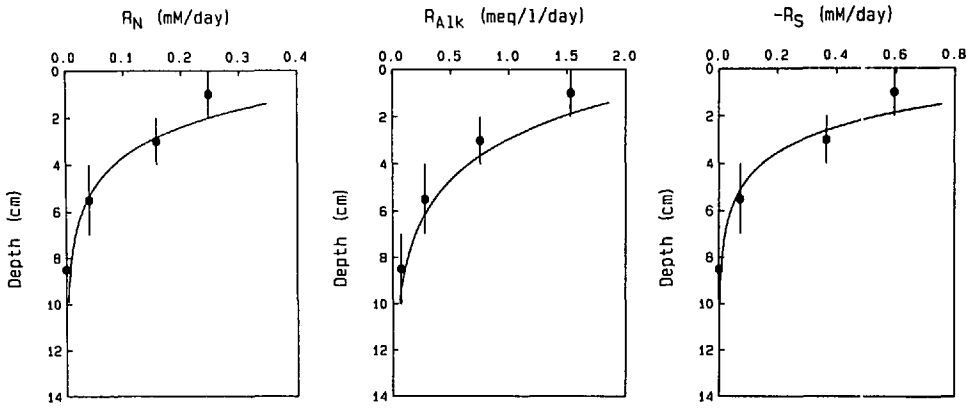

Figure 19. Comparison of estimated rates of NH_4^+ production, alkalinity production and $SO_4^=$ reduction from time series closed incubation of discrete sediment intervals (vertical bars over finite intervals) and the rate functions predicted from the whole core incubation profiles of Figure 18. The rate functions are NH_4^+: $R = 0.75 \exp(-0.55x)$; Alk = $3.25 \exp(-0.4x)$; and $SO_4^= = -2.0 \exp(-0.65x)$ mM/day with D_s = 0.869, 0.469, and 0.518 (HCO_3^-) cm^2/d respectively. Value of L = 10 cm; x in cm.

Figure 19. Good to excellent agreement between the two sets of rate (±20%) data imply that the treatment of whole-core incubation data described here provides good estimates of reaction rate distributions in surface nearshore sediments.

4. Discussion

Open-incubation diffusion techniques represent alternative methods of estimating the production/consumption rates of diffusible solutes in sediments. In some common circumstances, they give results comparable to those obtained by more established methods such as closed-incubation time series. The whole-core incubation technique in particular is a simple method for routine measurement of the magnitude and distribution of zeroth-order reaction rates in undisturbed sediments. It also has the obvious potential to be used for *in situ* rate determinations. Entombment of fauna can be a major problem for this method in productive sediments.

The plug-incubation technique allows ready examination of reaction kinetics. By altering diffusion scale-length, assumptions regarding concentration dependence and reaction functions can be investigated directly without change in substrate or sediment properties. In some cases growth of bacteria, microbial respiration, and adsorption/precipitation reactions in overlying water may compromise flux-based estimates of reaction rates. The spatial resolution and precision of the plug measurements is limited largely by sample volumes necessary for solute analyses. When a sensitive analytical technique is available, extremely small sediment plugs can be sampled; for example, near biogenic structures.

As illustrated by the Mn-reduction experiment, manipulation of pore water solute composition by changing boundary conditions or geometry without altering sediment fabric represents a major experimental potential of the plug-incubation technique. Production rates of strongly adsorbed species or species subject to authigenic mineral precipitation, like Mn^{++} and Fe^{++}, are also more readily studied by the plug-incubation technique because precipitation and adsorption reactions can be minimized by judicious choice of length scales. The dissolution of undersaturated mineral phases under conditions minimizing precipitation in open plug-incubations could also cause artifacts and multiple independent measurements of rates are generally required.

5. Conclusions

1. Net solute reaction rates in sediments can be readily estimated by exposing discrete intervals of sediments to an exchange reservoir, such as overlying sea water, and following solute concentration changes in each reservoir as a function of time. This 'plug' method is not restricted by availability of tracers and, in principle, can be used for any diffusing solute.

2. Steady-state, infinite reservoir approximations are often possible in the plug method, making calculations of reaction rate in sediments simple. In any case, exact finite reservoir models allow calculation of reaction constants and adsorption behavior from the time dependence of concentrations in each reservoir. Under some circumstances the method is insensitive and care is needed in determining optimal experimental conditions.

3. Nonsteady-state whole-core incubations allow calculation of reaction rate profiles for solutes subject to zeroth-order reactions (concentration independent). These incubations can be done *in situ*.

4. Comparison of open and closed incubations of varied scale-lengths allow evaluation of assumptions regarding the reaction kinetics governing particular solute production or consumption.

5. Manipulation of sediment thickness or reservoir boundary concentrations allow variation of specific solute concentrations in unamended sediments (no added substrates, no physical disturbance) and, in principle, separation of the interdependence of different reactions.

Acknowledgments. R. Nelson, S. Dougherty, and K. Swider aided in the field and laboratory. We thank the staff of the Belle Baruch Marine Laboratory (University of S. Carolina) where much of the field sampling was done. We also thank B. Boudreau for critical review. This research was supported mainly by NSF grant OCE-8613688 and various predecessors. Marine Sciences Research Center contribution 635.

APPENDIX I

Analytical solutions

The dimensionless solutions to Eqs. 1, 2, with conditions 3 and $R^* = R_1^*$ constant (definitions as in Eqs. 4) are:

$$C^*(x^*, t^*) = 1 + R_1^* t^* + \left[\frac{C_{To}^* - 1}{1 + V^*}\right] + \left[\frac{R_1^*(1/2 + V^*/6)}{(1 + V^*)^2}\right] - \left[\frac{R_1^*((x^* - 1)^2/2 + t^*)}{1 + V^*}\right] + \sum_{n=1}^{\infty}\left[\frac{(R_1^* + \alpha_n^2(C_{To}^* - 1))\cos(\alpha_n(x^* - 1))e^{-\alpha_n^2 t^*}}{\alpha_n^2 \Delta_n^*}\right]$$

$$C_T^*(t^*) = C_{To}^* + V^*\left[\frac{R_1^* t^*}{1 + V^*} - \sum_{n=1}^{\infty}\left[\frac{(R_1^* + \alpha_n^2(C_{To}^* - 1))\sin(\alpha_n)(e^{-\alpha_n^2 t^*} - 1)}{\alpha_n^3 \Delta_n^*}\right]\right]$$

where: α_n are the n real roots of

$$\alpha_n + V^* \tan(\alpha_n) = 0$$

and:

$$\Delta_n^* = \frac{1}{2}\left(V^* \cos(\alpha_n) - \alpha_n \sin(\alpha_n) - \frac{V^* \sin(\alpha_n)}{\alpha_n}\right)$$

$$n = 1, 2, 3, \ldots$$

The dimensional solutions are obtained by substitution of the definitions of Eqs. 4 into the dimensionless solutions.

When $C_T^* = C_{To}^*$ is constant ($V^* \to 0$; infinite overlying reservoir) then the dimensionless solution is simplified to:

$$C^*(x^*, t^*) = C_{To}^* + \frac{R_1^*}{2}(1 - (x^* - 1)^2) - 2\sum_{n=0}^{\infty}\left[\frac{(R_1^* + P_n^2(C_{To}^* - 1))(-1)^n \cos(P_n(x^* - 1))e^{-P_n^2 t^*}}{P_n^3}\right]$$

where: $P_n = (2n + 1)\pi/2$, $n = 0, 1, 2, \ldots$

The dimensionless solutions to Eqs. 1, 2, with conditions 3 and $R^* = k^*(1 - C^*)$ (definitions as in Eqs. 5) are:

$$C^*(x^*, t^*) = 1 + \frac{(C_{To}^* \mu^2 + (k^* - \mu^2)C_o^* - k^*)\cosh(\mu(x^* - 1))e^{(\mu^2 - k^*)t^*}}{\mu^2 \Delta_\mu^*} + \sum_{n=1}^{\infty}\frac{(C_{To}^* \alpha_n^2 + k^* - C_o^*(\alpha_n^2 + k^*))\cos(\alpha_n(x^* - 1))e^{-(\alpha_n^2 + k^*)t^*}}{\alpha_n^2 \Delta_n^*}$$

$$C_T^*(t^*) = C_{To}^* - V^*\left[\frac{(C_{To}^*\mu^2 + (k^* - \mu^2)C_o^* - k^*)\sinh(\mu)(e^{(\mu^2-k^*)t^*} - 1)}{(\mu^2 - k^*)\mu\Delta_\mu^*}\right]$$
$$- V^*\sum_{n=1}^{\infty}\left[\frac{(C_{To}^*\alpha_n^2 + k^* - C_o^*(\alpha_n^2 + k^*))\sin(\alpha_n)(e^{-(\alpha_n^2+k^*)t^*} - 1)}{(\alpha_n^2 + k^*)\alpha_n\Delta_n^*}\right]$$

where: μ is the real root of

$$V^*\mu\tanh(\mu) + \mu^2 - k^* = 0$$

α_n are the n real roots of

$$V^*\alpha_n\tan(\alpha_n) + \alpha_n^2 + k^* = 0$$

and

$$\Delta_\mu^* = \left(1 + \frac{V^*}{2}\right)\cosh(\mu) + (V^* + \mu^2 - k^*)\frac{\sinh(\mu)}{2\mu}$$
$$\Delta_n^* = \left(1 + \frac{V^*}{2}\right)\cos(\alpha_n) + (V^* - \alpha_n^2 - k^*)\frac{\sin(\alpha_n)}{2\alpha_n}.$$

The dimensional solutions are obtained by substitution of the definitions of Eqs. 5 into the dimensionless solutions.

When $C_T^* = C_{To}^*$ is constant ($V^* \to 0$; infinite overlying reservoir) then the dimensionless solution simplifies to:

$$C^*(x^*, t^*) = 1 + \frac{(C_{To}^* - 1)\cosh(\sqrt{k^*}(x^* - 1))}{\cosh(\sqrt{k^*})}$$
$$- 2\sum_{n=0}^{\infty}\left[\frac{(C_{To}^*P_n^2 - C_o^*(P_n^2 + k^*) + k^*)(-1)^n\cos(P_n(x^* - 1))e^{-(P_n^2+k^*)t^*}}{P_n(P_n^2 + k^*)}\right]$$

where: $P_n = (2n + 1)\pi/2$, $n = 0, 1, 2, \ldots$

The steady-state cases are obtained when $t^* \to$ large for both infinite reservoir solutions. The average dimensionless concentration in the sediment is obtained by integrating solutions over the interval $0 \le x^* \le 1$.

APPENDIX II

Numerical solution

For numerical evaluation of Eq. (1), the following approximations are made:

$$(\delta C/\delta t)_{x_i} \cong \frac{C(x_i, t_{j+1}) - C(x_i, t_j)}{\Delta t}$$

$$(\delta^2 C/\delta x^2)_{t_{j+1}} \cong \frac{C(x_{i-1}, t_{j+1}) - 2C(x_i, t_{j+1}) + C(x_{i-1}, t_{j+1})}{(\Delta x)^2}$$

where:

$$x_{i+1} = x_i + \Delta x; \quad x_{i-1} = x_i - \Delta x; \quad t_{j+1} = t_j + \Delta t.$$

Then, for each x_i, excluding $x = 0$ and $x = L$, Eq. (1) becomes:

$$\frac{C(x_i, t_{j+1}) - C(x_i, t_j)}{\Delta t} = D_s \frac{[C(x_{i+1}, t_{j+1}) - 2C(x_i, t_{j+1}) + C(x_{i-1}, t_{j+1})]}{(\Delta x)^2} + R_0 e^{-\alpha x_i} + R_1 \tag{II-1a}$$

Boundary conditions approximate to:

$$x = 0: \quad \frac{C(\Delta x, t_{j+1}) - C(0, t_{j+1})}{\Delta x} = 0 \tag{II-1b}$$

$$x = L: \quad \frac{C(L, t_{j+1}) - C(L - \Delta x, t_{j+1})}{\Delta x} = 0. \tag{II-1c}$$

Rearranging Eqs. (II-1) to place all t_{j+1} terms on the left-hand side, the following set of simultaneous equations is obtained:

$$x = 0: \quad C(\Delta x, t_{j+1}) - C(0, t_{j+1}) = 0$$

$$x = \Delta x \text{ to } x = L - \Delta x: \quad -D_s\beta C(x_{i-1}, t_{j+1}) + (1 + 2\beta)C(x_i, t_{j+1}) - D_s\beta C(x_{i+1}, t_{j+1}) = C(x_i, t_j) + (R_0 e^{-\alpha x_i} + R_1)\Delta t$$

$$x = L: \quad C(L, t_{j+1}) - C(L - \Delta x, t_{j+1}) = 0$$

where $\beta = \Delta t/(\Delta x)^2$.
Expressed in matrix form:

$$\mathbf{A}\mathbf{C}_{j+1} = \mathbf{C}_j + \mathbf{R}$$

or:

$$\mathbf{C}_{j+1} = \mathbf{A}^{-1}(\mathbf{C}_j + \mathbf{R}) \tag{II-2}$$

where $\mathbf{C}_{j+1}$ and $\mathbf{C}_j$ are vectors containing $n = L/\Delta x + 1$ concentrations at time t and time $t + \Delta t$, respectively, with the exception that the first and last elements of $\mathbf{C}_j = 0$ to satisfy boundary conditions. $\mathbf{R}$ is a vector with first and last elements = 0 (boundaries) and all other elements = $(R_0 e^{-\alpha x_i} + R_1)\Delta t$, and $\mathbf{A}$ is an $n \times n$ matrix having the following elements:

$$\mathbf{A}_{1,1} = \mathbf{A}_{n,n-1} = -1; \quad \mathbf{A}_{1,2} = \mathbf{A}_{n,n} = 1;$$

and, for $i = 2$ to $i = n - 1$: $\mathbf{A}_{i,i-1} = \mathbf{A}_{i,i+1} = -D_s\beta$;

$\mathbf{A}_{i,i} = 1 + 2D_s\beta$, with all other elements = 0.

In practice, matrix A is first inverted (see, e.g. Davis, 1973 for computed programming of matrix inversions; equations may also be solved by iteration methods) to give A^{-1}. Then, Eq. (II-2) is applied for each uniform time increment t until the total incubation time is obtained. The initial condition (23a) in the text gives the vector C_o, from which all other vectors C_j can be calculated. The parameters Δt and Δx are made arbitrarily small until the approximations (II-1) converge. Typical values for these parameters, using the depth and time-scales discussed in this paper, are $\Delta t = 0.1$–0.25 days and $\Delta x = 0.1$–0.25 centimeters.

REFERENCES

Aller, R. C. 1978. Experimental studies of changes produced by deposit feeders on pore water, sediment, and overlying water chemistry. Amer. J. Sci., *278*, 1185–1234.

—— 1980. Quantifying solute distributions in the bioturbated zone of marine sediments by defining an average microenvironment. Geochim. Cosmochim. Acta, *44*, 1955–1965.

Aller, R. C. and P. D. Rude. 1988. Complete oxidation of solid phase sulfides by manganese and bacteria in anoxic marine sediments. Geochim. Cosmochim. Acta, *52*, 751–765.

Aller, R. C. and J. Y. Yingst. 1980. Relationships between microbial distributions and the anaerobic decomposition of organic matter in surface sediments of Long Island Sound, U.S.A. Mar. Biol., *56*, 29–42.

Andrews, D. and A. Bennett. 1981. Measurements of diffusivity near the sediment-water interface with a fine-scale resistivity probe. Geochim. Cosmochim. Acta, *45*, 2169–2176.

Berner, R. A. 1976. Inclusion of adsorption in the modelling of early diagenesis. Earth Planet. Sci. Lett., *29*, 333–340.

—— 1980. Early Diagenesis. Princeton University Press, Princeton, NJ, 241 pp.

Blackburn, T. H. 1979. A method for measuring rates of NH_4^+ turnover in anoxic marine sediments using a $^{15}N - NH_4^+$ dilution technique. Appl. Environ. Microbiol., *37*, 760–765.

Boudreau, B. P. and N. L. Guinasso. 1980. The influence of a diffusive sublayer on accretion, dissolution and diagenesis at the seafloor, *in* The Dynamic Environment of the Ocean Floor, K. A. Fanning and F. T. Manheim, eds., Lexington Books, Lexington, MA, 115–145.

Burdige, D. J. and P. E. Kepkay. 1983. Determination of bacterial manganese oxidation rates in sediments using an *in situ* dialysis technique, I. Laboratory studies. Geochim. Cosmochim. Acta, *47*, 1907–1916.

Burdige, D. J. and K. H. Nealson. 1986. Chemical and microbiological studies of sulfide-mediated manganese reduction. Geomicrobio. J., *4*, 361–387.

Crill, P. M. and C. S. Martens. 1987. Biogeochemical cycling in an organic-rich coastal marine basin. 6. Temporal and spatial variations in sulfate reduction rates. Geochim. Cosmochim. Acta, *51*, 1175–1186.

Davis, J. C. 1973. Statistics and Data Analysis in Geology, J. Wiley and Sons, NY, 550 pp.

Goldhaber, M. B.., R. C. Aller, J. K. Cochran, J. K. Rosenfeld, C. S. Martens, and R. A. Berner. 1977. Sulfate reduction diffusion and bioturbation in Long Island Sound sediments: report of the FOAM group. Amer. J. Sci., *277*, 193–237.

Hurd, D. C. 1972. Factors affecting solution rate of biogenic opal in seawater. Earth Planet. Sci. Lett., *15*, 411–417.

Jahnke, R. A. 1988. A simple, reliable, and inexpensive pore water sampler. Limnol. Oceanogr., *33*, 483–487.

Jørgensen, B. B. 1977. The sulfur cycle of a coastal marine sediment (Linfjorden, Denmark). Limnol. Oceanogr., *22*, 814–831.

Keir, R. S. 1983. Variation in the carbonate reactivity of deep-sea sediments: determination from flux experiments. Deep-Sea Res., *30,* 279–296.

Kelly, J. R. 1983. Benthic-pelagic coupling in Narragansett Bay. Ph.D. dissertation. University of Rhode Island, Kingston, RI, 195 pp.

Krom, M. D. and R. A. Berner. 1980. Adsorption of phosphate in anoxic marine sediments. Limnol. Oceanogr., *25,* 797–806.

Li, Y.-H. and S. Gregory. 1974. Diffusion of ions in seawater and in deep-sea sediments. Geochim. Cosmochim. Acta, *38,* 703–714.

Mackin, J. E. 1987. Boron and silica behavior in salt-marsh sediments: implications for paleo-boron distributions and the early diagenesis of silica. Amer. J. Sci., *287,* 197–241.

Mackin, J. E. and R. C. Aller. 1984a. Ammonium adsorption in marine sediments. Limnol. Oceanogr., *29,* 250–257.

—— 1984b. Diagenesis of dissolved aluminum in organic-rich estuarine sediments. Geochim. Cosmochim. Acta, *48,* 299–313.

Martens, C. S. and R. A. Berner. 1974. Methane production in the interstitial waters of sulfate-depleted marine sediments. Science, *185,* 1167–1169.

McDuff, R. E. and R. A. Ellis. 1979. Determining diffusion coefficients in marine sediments: a laboratory study of the validity of resistivity techniques. Amer. J. Sci., *279,* 666–675.

Santschi, P. H., V. P. Nyffeler, P. O'Hara, M. Buchholtz and W. S. Broecker. 1984. Radiotracer uptake on the sea floor: results from the MANOP chamber deployments in the eastern Pacific. Deep-Sea Res., *29,* 953–965.

Schink, D. R., N. L. Guinasso, Jr. and K. A. Fanning. 1975. Processes affecting the concentration of silica at the sediment-water interface of the Atlantic Ocean. J. Geophys. Res., *80,* 3013–3031.

Ullman, W. J. and R. C. Aller. 1980. Dissolved iodine flux from estuarine sediments and implications for the enrichment of iodine at the sediment-water interface. Geochim. Cosmochim. Acta, *44,* 1177–1184.

—— 1982. Diffusion coefficients in nearshore marine sediments. Limnol. Oceanogr., *27,* 552–556.

—— 1983. Rates of iodine remineralization in terrigenous nearshore sediments. Geochim. Cosmochim. Acta, *47,* 1423–1432.

Received: *12 September, 1988;* revised: *24 January, 1989.*